THE MULTI-LAYERED RING UNDER PARABOLIC PRESSURE

Ch. F. Markides, E. D. Pasiou and S. K. Kourkoulis
National Technical University of Athens, Department of Mechanics,
Laboratory of Testing and Materials, Theocaris Building, Zografou Campus, 15773, Athens, Greece

1. Introduction

The configuration of a circular ring consisting of a finite number of concentric layers is commonly considered in a number of engineering applications, ranging from Biomechanics (human aorta) to Fluid Mechanics (insulated pipes). Such composite rings are usually loaded either by uniformly distributed internal or external pressure or by a combination of them. A more complicated loading mode appears when the ring is compressed between the curved jaws of the device suggested by ISRM [1] for the standardized implementation of the Brazilian-disc test. The ring is then under a cyclic distribution of radial stresses along two finite arcs of its periphery, which is accurately enough simulated by a parabolic scheme [2]. An attempt to determine analytically the stress- and displacement-fields developed in a ring consisting of three linearly elastic concentric layers, made up of different homogeneous and isotropic materials, under the as above loading scheme, is described here. A procedure analogous to Savin's one [3] for an infinite plate with a hole strengthened by rings (based on Muskhelishvili's complex potentials technique [4]) is adopted. The solution is extendable to rings of any number of layers. The analytic results are then considered in juxtaposition to those obtained numerically using the Finite Element Method.

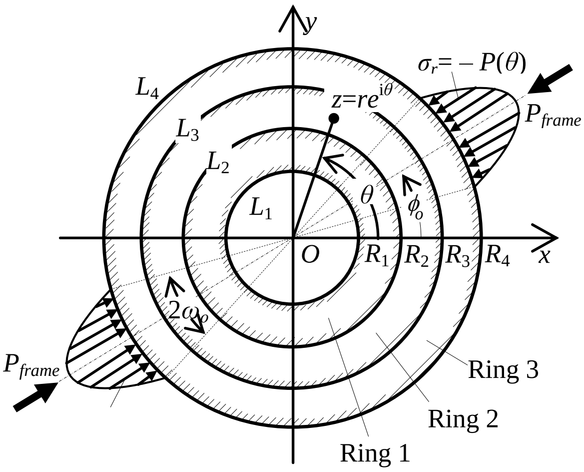

Fig. 1: Configuration of the problem.

2. Formulation of the problem, its analytic solution and the numerical simulations

The ring's cross-section is considered lying in the $z=x+iy=re^{i\theta}$ plane (Fig.1). R_j, R_{j+1}, j=1,2,3 are the inner and outer radii of the constituent rings with L_j, L_{j+1} being the respective boundaries. P_{frame} is the resultant force of the parabolic distribution imposed on two arcs of the L_4 boundary, each one of length $2R_4\omega_o$. The symmetry axis of P_{frame} forms an angle ϕ_o with x-axis. Assuming smooth contact between the ring and the jaws, the parabolic pressure, its altitude P_c and angle ω_o are written as [2]:

$$(1)\qquad \sigma_r^{(3)} = -P_c\left[1-\frac{sin^2(\phi_o-\phi)}{sin^2\omega_o}\right],\ \omega_o = \text{Arcsin}\sqrt{\frac{6K_3P_{frame}}{\pi R_4 w}},\ P_c=\sqrt{\frac{3\pi P_{frame}}{32K_3R_4w}},\ K_3=\frac{\kappa_3+1}{4\mu_3}+\frac{\kappa_J+1}{4\mu_J}$$

where w is the ring's thickness, $\kappa_3=3–4\nu_3$ and $\kappa_J=3–4\nu_J$ are Muskhelishvili's constants for plane strain conditions (ν is the Poisson's ratio) and μ_3, μ_J are the shear moduli of the outer layer and ISRM's jaw. The complex potentials for each j-constituent ring can be eventually put in the convenient form:

$$(2)\qquad \begin{aligned} \varphi^{(j)}(z) &= \alpha_1^{(j)}z + a_3^{(j)}z^3 + \sum_{k=4}^{\infty} a_k^{(j)}z^k + a_{-1}^{(j)}z^{-1} + \sum_{k=4}^{\infty} a_{-(k-2)}^{(j)}z^{-(k-2)} \\ \psi^{(j)}(z) &= b_1^{(j)}z + \sum_{k=4}^{\infty} b_{k-2}^{(j)}z^{k-2} + b_{-1}^{(j)}z^{-1} + b_{-3}^{(j)}z^{-3} + \sum_{k=4}^{\infty} b_{-k}^{(j)}z^{-k} \end{aligned}$$

$\alpha_1^{(j)}$ is a real constant while the remaining ones $a_{\pm k}^{(j)}$, $b_{\pm k}^{(j)}$ are complex constants. All of them are obtained by satisfying the boundary conditions for given stresses on L_1, L_4 and for welding conditions (i.e. action-reaction and common displacements) along L_2, L_3 ($a_2^{(j)}$, $b_{-2}^{(j)}$ turn to be zero). Stresses and displacements at any point of the ring are then provided by the well-known formulae [4]:

$$\sigma_\theta^{(j)} + \sigma_r^{(j)} = 4\Re\left[\varphi^{(j)\prime}(z)\right], \quad \sigma_r^{(j)} - \mathrm{i}\tau_{r\theta}^{(j)} = \varphi^{(j)\prime}(z) + \overline{\varphi^{(j)\prime}(z)} - e^{\mathrm{i}2\theta}\left[\bar{z}\,\varphi^{(j)\prime\prime}(z) + \psi^{(j)\prime}(z)\right]$$

$$u_r^{(j)} - \mathrm{i}u_\theta^{(j)} = \frac{e^{\mathrm{i}\theta}}{2\mu_j}\left[\kappa_j \overline{\varphi^{(j)}(z)} - \bar{z}\,\varphi^{(j)\prime}(z) - \psi^{(j)}(z)\right] \qquad (3)$$

The problem was then resolved numerically under plane strain conditions, using the ANSYS commercial software. For optimum simulation of the boundary conditions, both the ring and the jaws were modeled. The model was meshed with PLANE182 element. The three layers were considered perfectly bonded to each other. On the contrary, various friction coefficients f were considered along the ring-jaw interface, which was modeled using the CONTA171 and TARGE169 elements. The lower side of the lower jaw was clamped and a uniform displacement was imposed on the upper side of the upper jaw. Convergence analysis indicated that 60,000 elements provided sufficient accuracy. One quarter of the model is shown in Fig.2. The numerical data used are: R_n=15, 31, 35, 50 mm (n=1,2,3,4), E_γ=10, 2.1, 3.2 GPa, ν_γ=0.30, 0.38, 0.36 (γ=1,2,3). while for the jaws R_{jaw}=75 mm, E_{jaw}=210 GPa and ν_{jaw}=0.30.

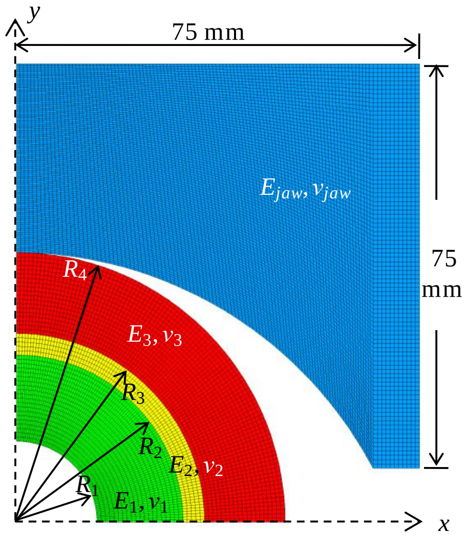

Fig. 2: The numerical model.

3. Results and conclusions

The data of the numerical solution for the variation of the $\sigma_{\theta\theta}$ stress along y-axis are plotted in Fig.3 for various values of f. In the same figure the results of the analytic solution are plotted. It is clear that the two approaches are quite close to each other and only in the immediate vicinity of the ring-jaw contact arc ($y\rightarrow R_4$) discrepancies appear for increased f-values (as it is expected, since the analytic solution assumed smooth contact). In general, the influence of friction becomes negligible as one moves away from the jaw. In addition it is noted that $\sigma_{\theta\theta}$ is of tensile nature for $y<R_4/2$ (maximized for $y=R_1$). Then $\sigma_{\theta\theta}$ decreases gradually becoming compressive. However, the maximum compressive stress (at $y=R_4$) is of the same order of magnitude with the tensile one, suggesting a kind of superiority of the ring-test against the respective compact-disc test, in which compression at the loaded rim exceeds by a large amount tension at the disc's center.

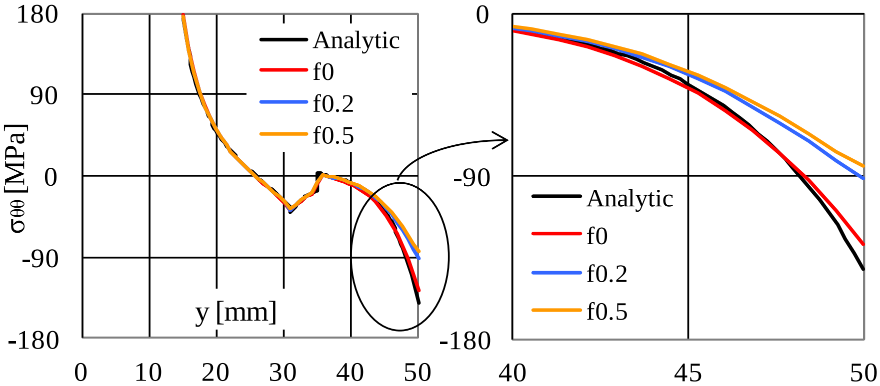

Fig. 3: Analytic and numerical results for the $\sigma_{\theta\theta}$ stress along y-axis (left) and a detailed view close to the ring-jaw contact arc (right).

4. References

[1] ISRM (1978). Suggested methods for determining tensile strength of rock materials. *Int. J. Rock Mech. Mining Sci. & Geomechanics Abs.*, **15(3)**, 99-103.

[2] S.K. Kourkoulis and Ch.F. Markides (2014). Stresses and displacements in a circular ring under parabolic diametral compression, *Int. J. Rock Mech. Min.*, **71**, 272–292.

[3] G.N. Savin (1961). *Stress Concentration Around Holes*. Pergamon Press, Oxford.

[4] N.I. Muskhelishvili (1963*). Some Basic Problems of the Mathematical Theory of Elasticity*, 4th ed. P. Noordhoff Groningen, Netherlands.